Dynamics of Beams Undergoing Large Rotations Accounting for Arbitrary Axial Deformation

Marcelo Areias Trindade* and Rubens Sampaio[†]
Pontifícia Universidade Católica do Rio de Janeiro, 22453-900 Rio de Janeiro, Brazil

It is well-known that flexible beams become stiffer when subjected to high-speed rotations. This is due to the membrane–bending coupling resulting from the large displacements of the beam cross section. This effect, often called geometric stiffening, has been largely discussed in the past two decades. Several methodologies have been proposed in the literature to account for the stiffening effect in the dynamics equations. However, considerable effort is generally expended to derive linear models using steady-state assumptions and membrane–bending decoupling. First a brief review of the open literature on this subject is presented. Then, a general nonlinear model is formulated using a nonlinear strain–displacement relation. This model is used to analyze deeply simplified models found in the literature. In particular, the assumption of steady-state values for the centrifugal load is analyzed, and its consequences are discussed. Thereafter, four finite element models are proposed, one based on nonlinear theory and the others on simplified linear theories. These models are then applied to the study of a flexible beam undergoing prescribed high-speed large rotations. The analyses show that one must account for the geometric stiffening effect to obtain realistic results. In addition, it is shown that models disregarding the axial displacement dynamics lead to erroneous results for the axial stress in the beam, which may be of primary importance in structural integrity analysis. Hence, in the general case, geometric stiffening must be accounted for in association with the inclusion of full axial–transverse displacements coupling dynamics in the model.

I. Introduction

THE dynamics and control of beams undergoing large rotations has received much attention in the past decade due to their wide applications in the aerospace, aviation, and robotic industries. However, the majority of the work reported in the open literature presents either only a refined model of the dynamics[1,2] or a specific controller design applied to a simple dynamics model.[3,4] The main complexity in modeling, and one of the most discussed topics in this literature, is the geometric stiffening due to rotation, which is also referred to as dynamic, centrifugal, or rotational stiffening. Moreover, as one should expect, controller design may be seriously ineffective if realistic models of the beam are not used.

Simo and Vu-Quoc[2] showed that the use of linear beam theory results in a spurious loss of stiffness due to the partial transfer of centrifugal force action to the bending equation. Hence, one should account for geometric stiffening due to large rotation of the base. To the authors' knowledge, the first study of vibration of rotating beams was published by Schilhansl,[5] who analyzed the bending vibration, assuming steady-state revolution and negligible Coriolis force. He derived a formula relating the fundamental bending eigenfrequency with the angular velocity of revolution.

Several methodologies for incorporating the stiffening effect into the dynamics were reviewed by Sharf[6] and are still studied today.[7] Kane et al.[1] observed that previous multibody formulations did not account properly for the geometric stiffening effect. They proposed an alternative methodology using higher-order strain measures and applied it to the dynamics of a cantilever beam attached to a moving base under prescribed large translation and rotation. Padilla and von

Flotow[8] noted that the error of previous formulations was due to a premature linearization of the displacement field. Later, Hanagud and Sarkar[9] observed that the formulation proposed by Kane et al.[1] was inconsistent and pointed out that, contrary to the Kane et al. observation, the stiffening effect can be accounted for using nonlinear strain–displacement relations. In fact, contrary to London's comment,[10] the formulation used by Kane et al.[1] implicitly includes a nonlinear strain–displacement relation, which is not apparent due to the choice of independent variables employed. The analysis for a cantilever beam by Kane et al.[1] was later extended to an arbitrary flexible body in a work by Banerjee and Dickens,[11] in which the authors evaluate the geometric stiffness from prescribed loads representing the inertia forces and couples acting throughout the body.

Simo and Vu-Quoc[2] applied their theory of geometrically nonlinear beams to the case of a rotating beam. Their formulation also accounted for shear strains in the beam. However, their "consistent" linearization using the steady-state value for the axial internal force has led to equivalent equations as compared to those of transverse vibrations of beams subjected to a steady-state centrifugal load.[12] Oguamanam and Heppler[13] also accounted for shear strains to derive the equations of motion of a rotating Timoshenko beam with a tip mass. Wallrapp and Schwertassek[14] preferred to account for the geometric stiffening through the use of a reference stress treated as an initial stress in the undeformed configuration. Recently, a generalization of the cantilever beam foreshortening to other structural members was proposed by Urruzola et al.[15] A more complete review oriented to multibody systems may be found in a recent paper by Sharf.[6] However, modeling of geometric stiffening effects has induced interest in several other areas dealing with flexible structures undergoing large displacements and rotations, such as long satellite appendages and submerged cables.

In the next sections, a general nonlinear model is formulated using a nonlinear strain–displacement relation. Through a variational formulation, nonlinear equations of motion are developed and used to derive the cited simplified models previously proposed in the literature. Then, one nonlinear and three linear simplified finite element models are presented and applied to the study of the dynamics of a flexible beam undergoing prescribed high-speed large rotations. The results of the four models are compared in terms of representation of axial and transverse displacements dynamics behavior and the axial stress induced in the beam.

*Postdoctoral Research Assistant, Department of Mechanical Engineering, rua Marquês de São Vicente, 225; trindade@mec.puc-rio.br. Member AIAA.
†Professor, Department of Mechanical Engineering, rua Marquês de São Vicente, 225; rsampaio@mec.puc-rio.br.
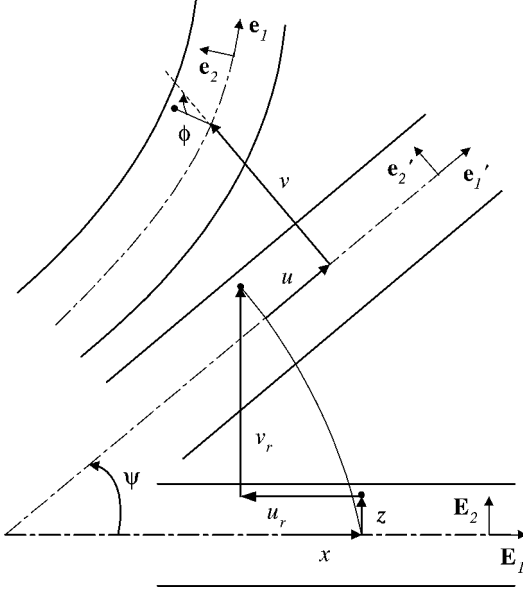
Fig. 1   Beam undergoing large plane rotation and small deformation.

II.   Nonlinear Model Formulation

Let us consider a straight beam, of undeformed length L and thickness h, undergoing large plane rotation and small deformation as shown in Fig. 1. The beam rotation is represented by a prescribed time-dependent rotation angle ψ and defines the floating frame $\mathbf{e}'_i \otimes \mathbf{e}'_j$ (also known as locally attached frame) with respect to the inertial frame $\mathbf{E}_i \otimes \mathbf{E}_j$.

A.   Displacements and Strain Measures

Small deformations are assumed so that the beam cross-sectional rotation angle ϕ is small. Consequently, the position vectors $\mathbf{X}$ and $\mathbf{x}$ of a given point in the undeformed and deformed configurations are, respectively,

$$\mathbf{X} = \begin{bmatrix} x \\ z \end{bmatrix}, \qquad \mathbf{x} = \begin{bmatrix} x - u_r + (u + z\phi)\cos\psi - v\sin\psi \\ z + v_r + (u + z\phi)\sin\psi - v\cos\psi \end{bmatrix} \quad (1)$$

where x and z are components of the undeformed position vector, such that $0 \le x \le L$ and $-h/2 \le z \le h/2$. Also, the assumption of negligible shear strains, leading to $\phi = -v'$, is considered. Note that the prime denotes the derivative with respect to the axial coordinate x.

The rotation operator $\mathbf{R}$, defined from $\mathbf{e}'_i = \mathbf{R}^T \mathbf{E}_i$, is

$$\mathbf{R} = \begin{bmatrix} \cos\psi & -\sin\psi \\ \sin\psi & \cos\psi \end{bmatrix} \quad (2)$$

Hence, the position vector $\mathbf{x}_r = \mathrm{col}(x - u_r, z + v_r)$ after the rigid rotation is clearly $\mathbf{x}_r = \mathbf{R}\mathbf{X}$ and the total displacement vector $\mathbf{p}_T = \mathbf{x} - \mathbf{X}$ may be written as

$$\mathbf{p}_T = \mathbf{R}\mathbf{p} + (\mathbf{R} - \mathbf{I})\mathbf{X} \quad (3)$$

where

$$\mathbf{p} = \begin{bmatrix} u - zv' \\ v \end{bmatrix} \quad (4)$$

where v' stands for $\mathrm{d}v/\mathrm{d}x$. The deformation gradient $\mathbf{F}$ relative to the reference position is defined as

$$\mathbf{F} = \frac{\mathrm{d}\mathbf{x}}{\mathrm{d}\mathbf{X}} = \mathbf{R}\left(\frac{\mathrm{d}\mathbf{p}}{\mathrm{d}\mathbf{X}} + \mathbf{I}\right) \quad (5)$$

and the Lagrangian strain tensor $\mathbf{E}$ is

$$\mathbf{E} = \frac{1}{2}(\mathbf{F}^T\mathbf{F} - \mathbf{I}) = \frac{1}{2}\left[\left(\frac{\mathrm{d}\mathbf{p}}{\mathrm{d}\mathbf{X}}\right) + \left(\frac{\mathrm{d}\mathbf{p}}{\mathrm{d}\mathbf{X}}\right)^T + \left(\frac{\mathrm{d}\mathbf{p}}{\mathrm{d}\mathbf{X}}\right)^T\left(\frac{\mathrm{d}\mathbf{p}}{\mathrm{d}\mathbf{X}}\right)\right] \quad (6)$$

where

$$\left(\frac{\mathrm{d}\mathbf{p}}{\mathrm{d}\mathbf{X}}\right) = \begin{bmatrix} u' - zv'' & -v' \\ v' & 0 \end{bmatrix} \quad (7)$$

Here, only the axial component of the strain tensor $\varepsilon_{xx} \equiv E_{11}$ is considered. Therefore, defining the axial displacement as $u_0 = u - zv'$, the nonlinear axial strain ε_{xx} may be written in the following form:

$$\varepsilon_{xx} = u'_0 + \tfrac{1}{2}\left[(u'_0)^2 + (v')^2\right] \quad (8)$$

B.   Strain and Kinetic Energies

From the assumption of negligible shear strains and also neglecting the contribution of transverse normal stress σ_{zz}, the potential energy of the beam is

$$H = \frac{1}{2}\int E\varepsilon_{xx}^2 \, \mathrm{d}V \quad (9)$$

where E is Young's modulus of the beam. When a symmetric beam cross section with respect to z axis is considered and the axial strain definition (8) is used, the potential energy [Eq. (9)] of the beam may be written in terms of the mean axial u and transverse v displacements only. Thus,

$$H = \frac{1}{2}\int_0^L \left[EA\left(u'^2 + u'v'^2 + \frac{1}{4}v'^4 + u'^3 + \frac{1}{4}u'^4 + \frac{1}{2}u'^2v'^2\right) \right.$$
$$\left. + EI\left(v''^2 + 3u'v''^2 + \frac{3}{2}u'^2v''^2 + \frac{3h^2}{20}v''^4 + \frac{1}{2}v'^2v''^2\right) \right]\mathrm{d}x \quad (10)$$

where A and I are the area and moment of inertia of the beam cross section. Single-underlined terms in Eq. (10) are due to the presence of $(v')^2$, quadratic in the cross-sectional rotation angle $\phi = -v'$, in the axial strain ε_{xx}. Note that they appear only in the membrane strain component, unlike the double- and triple-underlined terms that are present in both membrane and bending components of the strain energy. The term $(u'_0)^2$, quadratic in the axial displacement derivative, of the axial strain [Eq. (8)] leads to the double-underlined terms in the strain energy function, while triple-underlined terms are due to the coupling between the two quadratic terms of the axial strain. Also note that the assumption of the linear strain–displacement relation eliminates all underlined terms of Eq. (10).

The kinetic energy of the beam may also be written in terms of the main variables u and v. Thus, starting from the following general form of the kinetic energy in terms of the total displacement of the beam, one obtains

$$T = \frac{1}{2}\int \rho \dot{\mathbf{p}}_T^T \dot{\mathbf{p}}_T \, \mathrm{d}V \quad (11)$$

where ρ is the beam mass density and $\dot{\mathbf{p}}_T$ is the velocity vector of a given point $\mathbf{X}$ of the beam, which, from Eq. (3), may be written as $\dot{\mathbf{p}}_T = \dot{\mathbf{R}}(\mathbf{p} + \mathbf{X}) + \mathbf{R}\dot{\mathbf{p}}$. Then, when the definitions of $\mathbf{p}$ [Eq. (4)] and $\mathbf{R}$ [Eq. (2)] are used and a symmetric beam cross section with respect to the z axis is assumed, the kinetic energy of the beam may be written in terms of the main variables u and v as

$$T = \frac{1}{2}\int_0^L \{\rho A[\dot{u}^2 + \dot{v}^2 + 2\dot{\psi}(\dot{v}u - \dot{u}v + \dot{v}x) + \dot{\psi}^2(u^2 + v^2$$
$$+ 2ux + x^2)] + \rho I[\dot{v}'^2 + 2\dot{\psi}\dot{v}' + \dot{\psi}^2(1 - v'^2)]\}\,\mathrm{d}x \quad (12)$$

where terms of zero order in $\dot{\psi}$ correspond to translation, in the x and z directions, and rotation inertias due to beam deformation.

C.   Nonlinear Equations of Motion

Using the expressions for strain [Eq. (10)] and kinetic [Eq. (12)] energies presented earlier, a variational formulation is used to write the equations of motion. Hence, from Hamilton's principle,

$$\delta \int_{t_1}^{t_2} (T - H)\,\mathrm{d}t = 0 \quad (13)$$

the fully nonlinear equations of motion may be written in terms of the main variables u and v as

$$\rho A[\ddot{u} - 2\dot{\psi}\dot{v} - \dot{\psi}^2(u+x) - \ddot{\psi}v] - EA\big(u'' + v'v'' + 3u'u''$$

$$+ \tfrac{3}{2}u'^2u'' + \tfrac{1}{2}u''v'^2 + u'v'v''\big)$$

$$- EI\big(3v''v''' + \tfrac{3}{2}u''v''^2 + 3u'v''v'''\big) = 0 \qquad (14a)$$

$$\rho A[\ddot{v} + 2\dot{\psi}\dot{u} - \dot{\psi}^2 v + \ddot{\psi}(u+x)] - \rho I(\ddot{v}'' + \dot{\psi}^2 v'') + EI\big(v''''$$

$$+ 3u'''v'' + 6u''v''' + 3u'v'''' + 3u''^2 + 6u'u''v'' + 3u'u'''v''$$

$$+ \tfrac{3}{2}u'^2v'''' + \tfrac{1}{2}v'^2v'''' + 2v'v''v''' + \tfrac{1}{2}v''^3\big) - EA\Big(\underline{u''v' + u'v''}$$

$$+ \tfrac{1}{2}u'^2 + u'u''v' + \underline{\tfrac{3}{2}v'^2v''}\Big) = 0$$

$$(14b)$$

Note that the inertial terms in Eq. (14) are composed of 1) inertia forces, due to beam deformation with respect to the reference configuration; 2) gyroscopic or Coriolis forces, caused by the rotation of the reference frame with respect to the inertial one; and 3) centrifugal and tangential forces, due to centrifugal and tangential accelerations of the reference frame. The other terms correspond to the material membrane and bending stiffness. Note also that some of the terms due to centrifugal and tangential acceleration of the reference frame are linear functions of axial and transverse displacements. That is why they may also be interpreted as dynamic geometric stiffness terms.

III. Simplified Models

In this section, two linear models are obtained through linearization of equations of motion (14). The first model is constructed by neglecting all nonlinear terms in Eq. (14), which corresponds to the assumption of a linear strain–displacement relation. The second model is based on a common assumption of steady-state values for the axial displacement, leading to a linear model in the transverse displacement v.

A. Linearization of Equations of Motion

A set of linear equations of motion corresponding to the rotating beam may be obtained by linearization of system (14). This leads to

$$\rho A[\ddot{u} - 2\dot{\psi}\dot{v} - \dot{\psi}^2(u+x) - \ddot{\psi}v] - EAu'' = 0 \qquad (15a)$$

$$\rho A[\ddot{v} + 2\dot{\psi}\dot{u} - \dot{\psi}^2 v + \ddot{\psi}(u+x)] - \rho I(\ddot{v}'' + \dot{\psi}^2 v'') + EIv'''' = 0$$

$$(15b)$$

It can be shown that the linearization yielding these equations of motion is equivalent to the assumption of a linear strain–displacement relation. This is done by considering only the first term in the axial strain definition (8) or, alternatively, neglecting all underlined terms in the strain–energy function (10).

However, these equations do not represent correctly the physically expected bending stiffening effect due to beam rotation. Better understanding may be achieved through a bending frequency analysis of the linear system (15), considering a constant angular velocity of the beam ($\ddot{\psi} = 0$) and negligible rotation inertia of the beam cross section. Hence, when harmonic motion $v(t, x) = \beta(x)e^{j\omega t}$ is supposed, Eq. (15b) may be written as

$$EI\beta'''' - \rho A(\omega^2 + \dot{\psi}^2)\beta = 0 \qquad (16)$$

where the general solution of Eq. (16) is in the form $\beta(x) = Ce^{\lambda x/L}$, leading to the roots $\lambda = \pm\mu, \pm j\mu$, for which corresponding coefficients C_i are evaluated from boundary conditions. Then, for each vibration mode, the equivalent frequency may be evaluated by

$$\omega^2 = (EI/\rho AL^4)\mu^4 - \dot{\psi}^2 \qquad (17)$$

Note that the first term on the right-hand side of Eq. (17) is the natural frequency expression for the nonrotating beam. Consequently,

from Eq. (17), the natural frequency for the rotating beam ω decreases with the angular velocity, such that for some critical value of $\dot{\psi}_c = (\mu/L)^2 \sqrt{(EI/\rho A)}$ the bending frequency corresponding to μ vanishes. This can be interpreted as loss of bending stiffness, quadratic in the angular velocity, due to the lack of stiffening terms in the model. In fact, when the angular velocity reaches some of its critical values $\dot{\psi}_c$, the bending stiffness operator becomes singular.

However, we think that it is not appropriate to denote the term $-\dot{\psi}^2 v$ as a destiffening or softening term because it is due to the centrifugal forces caused by the beam rotation. Indeed, the presence of this term is independent of the strain–displacement relation assumption because it comes from the kinetic energy. The loss of stiffness is actually due to the incoherence in modeling a rotating beam, that is, subjected to large displacements, without accounting for the geometric stiffness terms.

B. Inclusion of Geometric Stiffening Terms

In the preceding subsection, it was shown that, to account for the geometric stiffening due to beam rotation, it is necessary to include nonlinear terms in the strain–displacement relation. Simo and Vu-Quoc[2] consider including an extra term, $-[\rho A\dot{\psi}^2(L^2 - x^2)/2v']'$, in linearized equation (15b) corresponding to the transverse displacement v. This is equivalent to using the assumption of steady-state values for the axial displacement u, which is commonly used in the literature.[6] This is done by keeping only the first of the single-underlined terms and neglecting all other underlined terms in the strain energy function (10). Then, the energy resulting from the remaining underlined term is interpreted as the work done by a centrifugal load $P = EAu'$, such that

$$H = \frac{1}{2}\int_0^L (EAu'^2 + EIv''^2)\,dx + \frac{1}{2}\int_0^L Pv'^2\,dx \qquad (18)$$

The centrifugal force $P(x)$ may be interpreted as an axial load applied at a given point x of the beam due to the rotation inertia of the section $[x, L]$. In addition, the centrifugal force P is assumed time independent, so that it can be approximated by its steady-state value, written as[6]

$$P(x) = \tfrac{1}{2}\rho A\dot{\psi}^2(L^2 - x^2) \qquad (19)$$

Then, the virtual variation of strain energy H leads to an additional term in the equations of motion, that is, $-(Pv')'$, which is the same as that presented by Simo and Vu-Quoc.[2]

The main advantage of such assumption is that it leads to additional terms that are linear in v, and consequently, the resulting equations of motion are linear. However, this assumption is only valid for steady-state centrifugal loads and, thus, steady-state axial displacements. Therefore, equations of motion resulting from this assumption should only have the transverse displacement equation (15b). To provide better understanding, let us analyze the origin of this assumption. From Eq. (15a) and assuming time-independent ($\dot{u} = \ddot{u} = 0$) and small ($u \ll x$) axial displacement, one gets

$$\rho A\dot{\psi}^2 x + EAu'' = 0 \qquad (20)$$

which, together with boundary conditions $u(0) = 0$ and $u'(L) = 0$, leads to the following expression for the steady-state axial displacement:

$$u(x) = (\rho\dot{\psi}^2/6E)(3L^2 x - x^3) \qquad (21)$$

It is clear that this expression for u is equivalent to Eq. (19) because $P = EAu'$.

It is, thus, worthwhile to restart from Eqs. (14), using the same assumptions as earlier, that is, steady state and small axial displacement. Notice that to consider only the work done by the centrifugal load P is equivalent to neglecting all nonlinear terms in Eq. (14) except for the first two underlined terms in Eq. (14b). Also, from the assumptions for the axial displacement u, Eq. (14a) reduces clearly

to Eq. (20). Hence, in contrast to what was stated by other authors, these assumptions on axial displacement imply Eq. (14a) is identical to Eq. (20). Moreover, when rotation inertia of the cross section is neglected, Eq. (14b) reads

$$\rho A(\ddot{v} - \dot{\psi}^2 v) + E I v'''' - E A(u''v' + u'v'') = 0 \qquad (22)$$

Then, substituting the steady-state value for $u(x)$ [Eq. (21)] in the last expression, one obtains

$$\rho A\left\{ \ddot{v} - \dot{\psi}^2 \left[v - xv' + \tfrac{1}{2}(L^2 - x^2)v'' \right] \right\} + E I v'''' = 0 \qquad (23)$$

This expression is equivalent to Eq. (3) by Simo and Vu-Quoc.[2] However, contrary to what is stated by these authors, Coriolis force due to rotation $(2\dot{\psi}\dot{u})$ should not appear in this equation because $\dot{u}$ is assumed to vanish.

An analysis of the effect of terms due to $\dot{\psi}^2$ in Eq. (23) may be carried out by using the approach already employed in the work of Schilhansl.[5] Hence, one can assess precisely the stiffening caused by rotation.

Let us assume the following harmonic solution for the transverse displacement:

$$v = \beta(x)e^{j\omega t} \qquad (24)$$

then, Eq. (23) may be rewritten as

$$\beta'''' = \rho A/E I \left[(\omega + \dot{\psi}^2)\beta + \dot{\psi}^2 x\beta' - \tfrac{1}{2}\dot{\psi}^2(L^2 - x^2)\beta'' \right] \qquad (25)$$

A first approximation $\beta_0(x) = 6L^2 x^2 - 4Lx^3 + x^4$ is done, respecting all geometrical and dynamic boundary conditions for a cantilever beam, that is, zero displacement $\beta = 0$ and rotation $\beta' = 0$ at $x = 0$ and zero bending moment $\beta'' = 0$ and shear force $\beta''' = 0$ at $x = L$. Thereafter, the expression for $\beta_0(x)$ is introduced in the right-hand side of Eq. (25), leading to

$$\beta_1'''' = \rho A/E I[(\omega^2 - 9\dot{\psi}^2)x^4 - 4L(\omega^2 - 5\dot{\psi}^2)x^3$$
$$+ 6L^2(\omega^2 - \dot{\psi}^2)x^2 - 12\dot{\psi}^2 L^3 x + 6\dot{\psi}^2 L^4] \qquad (26)$$

The updated function $\beta_1(x)$ is obtained by integrating the last equation four times and satisfying geometric and dynamic boundary conditions. Then, the best agreement of functions $\beta_0(x)$ and $\beta_1(x)$ is reached by the requirement that

$$\int_0^L \beta_0(x)\,dx = \int_0^L \beta_1(x)\,dx \qquad (27)$$

Solving this equation for ω^2 leads to the following expression of the natural frequency ω in terms of the angular velocity $\dot{\psi}$:

$$\omega^2 = \left(\tfrac{162}{13}\right)(E I/\rho A L^4) + \left(\tfrac{9}{52}\right)\dot{\psi}^2 \qquad (28)$$

where the first term is an approximation (under 1% error) to the first natural bending frequency of a nonrotating beam. The second term states the increase in frequency, and thus in stiffness, due to the beam rotation. The coefficient $\tfrac{9}{52}$ for $\dot{\psi}^2$, the so-called Southwell coefficient, matches exactly that presented by Schilhansl.[5]

Figure 2 shows the first natural frequency ω, normalized with respect to the exact natural frequency for a nonrotating beam $\omega_e = 1.85^4 E I/(\rho A L^4)$, in terms of the angular velocity $\dot{\psi}$ for several beam thicknesses, $h = 0.1, 0.3, 1, 2,$ and 10 mm. The material and geometrical properties considered are $E = 71$ GPa, $\rho = 2710$ kg m^{-3}, and $L = 500$ mm.

In Fig. 2, note that the linearized model (dashed lines) does not account for geometric stiffening and, as shown earlier, yields a reduction in the natural frequency as the angular velocity augments. Consequently, for thin beams ($h = 0.1$ and 0.3 mm), an angular velocity of 10 rad/s is sufficient to nullify the natural frequency. On the other hand, the model assuming steady-state axial displacement (solid lines in Fig. 2) well represents the increase in frequency due to beam rotation. Moreover, the influence of angular velocity in natural frequency varies with beam thickness. This effect is also presented in Fig. 2, showing that as the beam thickness increases
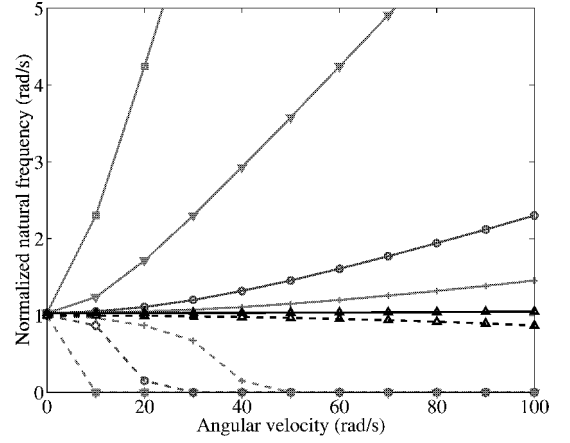
Fig. 2   Normalized natural frequency in terms of angular velocity, using linearized model (17) (- - -) and steady-state model (28) (——); for several beam thicknesses: □, 0.1 mm; ▽, 0.3 mm; ○, 1 mm; +, 2 mm; and △, 10 mm.

the influence of angular velocity on frequency diminishes. This may be because the beam stiffness increases with its thickness; hence, higher centrifugal loads, and thus angular velocities, are necessary to induce a change in the natural frequencies. According to these results, it is conjectured that the effect of geometric stiffening would be important mainly for the lowest natural frequencies of slender beams. This is in agreement with the Euler–Bernoulli assumption considered here.

From the preceding results, one would be tempted to keep only the first two underlined nonlinear terms in Eq. (14b) together with the assumptions on u to obtain the uncoupled equation (23) in the transverse displacement. Indeed, this would be sufficient to capture the geometric stiffening due to rotation. However, this is only valid for steady-state axial displacement, and it is clear that this would only be realistic for constant angular velocity $\dot{\psi}$ and in the presence of damping to dissipate axial displacement due to initial angular acceleration. Also note that, for time-varying axial displacement, it would be difficult to analyze the stiffening effect because bending stiffness would increase or decrease accompanying the centrifugal load P and, thus, the axial displacement u. Hence, for the general case, one should keep both nonlinear equations (14a) and (14b) without the assumptions on u to eliminate this variable from Eq. (14b).

A simpler alternative to the nonlinear model (14) may be obtained by neglecting the strain energy contributions due to the term $(u'_0)^2$ in the strain–displacement relation, which is generally done in the small deformation/large displacements approach. However, for this special case of the rotating beam, one should agree that, for large enough angular velocities, axial strains u'_0 may not be negligible compared to v'.

IV.   Finite Element Models

In this section, one nonlinear and three simplified linear finite element models for beams are developed. They were obtained using the simplifying assumptions presented in preceding sections.

A.   Nonlinear Finite Element

The first finite element model [nonlinear (NL)] is constructed through discretization of strain [Eq. (10)] and kinetic [Eq. (12)] energies, considering only the first single-underlined term of Eq. (10), that is, $E A u'v'^2$. It is clear that neglecting the other underlined terms in the strain energy leads to the absence of several terms in the full nonlinear model (14). However, it is expected that the geometric stiffening aspect may be correctly accounted for by the resulting term, $E A(u''v' + u'v'')$. The discretization is carried out using Lagrange linear shape functions for the axial displacement u and Hermite cubic ones for the transversal deflection v. This leads to six degrees of freedom, $q^T = [u_1, v_1, \beta_1, u_2, v_2, \beta_2]$, where $(\beta_1, \beta_2) = (v'_1, v'_2)$. Using Hamilton's principle [Eq. (13)], combined

with the discretized strain and kinetic energies, leads to the following equations of motion:

$$(M_t + M_r)\ddot{q} + G\dot{q} + [K_e + K_g(q) + K_v + K_a]q = F_v + F_a \quad (29)$$

where $\dot{q}$ and $\ddot{q}$ are the velocity and acceleration vectors and the symmetric translation and rotation inertia matrices M_t and M_r are

$$M_t = \frac{\rho A L}{420} \begin{bmatrix} 140 & 0 & 0 & 70 & 0 & 0 \\ & 156 & 22L & 0 & 54 & -13L \\ & & 4L^2 & 0 & 13L & -3L^2 \\ & & & 140 & 0 & 0 \\ & \text{sym} & & & 156 & -22L \\ & & & & & 4L^2 \end{bmatrix}$$

$$M_r = \frac{\rho I}{L} \begin{bmatrix} 0 & 0 & 0 & 0 & 0 & 0 \\ & 6/5 & 1/10L & 0 & -6/5 & 1/10L \\ & & 2/15L^2 & 0 & -1/10L & -1/30L^2 \\ & & & 0 & 0 & 0 \\ & \text{sym} & & & 6/5 & -1/10L \\ & & & & & 2/15L^2 \end{bmatrix} \quad (30)$$

The stiffness of the beam is composed of four contributions. The symmetric elastic stiffness matrix K_e corresponds to the standard Euler–Bernoulli beam with axial and bending stiffness. K_g is the geometric stiffness, which as already presented depends on the configuration and, thus, corresponds to nonlinear terms in the equations of motion. K_v and K_a correspond to the stiffness induced by the rotation of the beam, where the first one is symmetric and proportional to the square of the rotation velocity and the second one antisymmetric and proportional to the angular acceleration. These stiffness matrices are

$$K_e = \frac{E}{L} \begin{bmatrix} A & 0 & 0 & -A & 0 & 0 \\ & 12I/L^2 & 6I/L & 0 & -12I/L^2 & 6I/L \\ & & 4I & 0 & -6I/L & 2I \\ & & & A & 0 & 0 \\ & \text{sym} & & & 12I/L^2 & -6I/L \\ & & & & & 4I \end{bmatrix}$$

$$K_a = \rho A L \ddot{\psi} \begin{bmatrix} 0 & -7/10 & -1/10L & 0 & -3/10 & 1/15L \\ & 0 & 0 & 3/10 & 0 & 0 \\ & & 0 & 1/15L & 0 & 0 \\ & & & 0 & -7/10 & 1/10L \\ & \text{antisym} & & & 0 & 0 \\ & & & & & 0 \end{bmatrix} \quad (31)$$

Notice that the geometric stiffness matrix K_g depends on the variables $\tilde{u} = u_2 - u_1$, $\tilde{v} = v_2 - v_1$ and $\bar{\beta} = \beta_1 + \beta_2$. Moreover, the bending stiffness $2/15EA\tilde{u}$ varies linearly with the relative axial displacement $\tilde{u}$. That is, this stiffness increases when $\tilde{u}$ is positive and decreases in the opposite case. This is in agreement with the notion that the beam is stiffer when under extension and that it loses stiffness when under axial compression.

The gyroscopic matrix G, corresponding to Coriolis forces, is proportional to the rotation velocity and leads to exchange of energy between axial and transversal motions. The rotation of the beam leads also to applied forces F_v and F_a proportional to the square of the angular velocity and to the angular acceleration, respectively. Thus,

$$G = \rho A L \dot{\psi} \begin{bmatrix} 0 & -7/10 & -1/10L & 0 & -3/10 & 1/15L \\ & 0 & 0 & 3/10 & 0 & 0 \\ & & 0 & 1/15L & 0 & 0 \\ & & & 0 & -7/10 & 1/10L \\ & \text{antisym} & & & 0 & 0 \\ & & & & & 0 \end{bmatrix}$$

$$F_v = \rho A L^2 \dot{\psi}^2 \begin{bmatrix} 1/6 \\ 0 \\ 0 \\ 1/3 \\ 0 \\ 0 \end{bmatrix}, \qquad F_a = \rho \ddot{\psi} \begin{bmatrix} 0 \\ -3/20AL^2 + I \\ -1/30AL^3 \\ 0 \\ -7/20AL^2 - I \\ 1/20AL^3 \end{bmatrix} \quad (34)$$

Note that the applied force vector F_v, proportional to the square of the angular velocity, represents a centrifugal load in the beam axial direction. The force vector F_a, proportional to the angular acceleration, leads to bending in the beam.
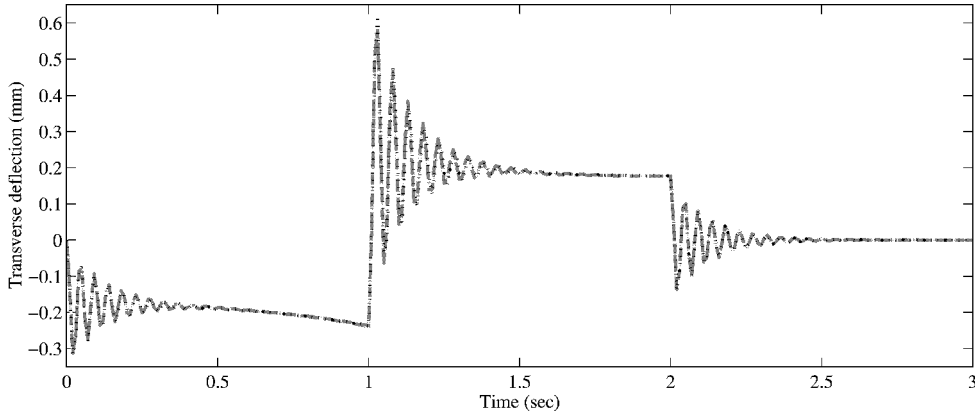
B. Linearized Finite Element

The second finite element model [linear with both u and v as variables (Luv)] is obtained from the NL model presented in the preceding section but neglecting the geometric stiffening term. This leads to a finite element model corresponding to the linearized equations of motion (15). Hence, the resulting discretized equations of motion are equivalent to the nonlinear Eq. (29) without the geometric stiffness matrix K_g:

$$(M_t + M_r)\ddot{q} + G\dot{q} + (K_e + K_v + K_a)q = F_v + F_a \quad (35)$$

Notice that, because K_g is the only nonlinear term in Eq. (29), the equations for the present Luv finite element [Eq. (35)] are linear in q. Nevertheless, the axial and transverse displacements are still coupled.

C. Finite Element for Beams Subjected to Axial (Centrifugal) Loads

The third finite element model considered [centrifugal loads with only v as variable (CLv)] describes the transverse vibrations of

$$K_g = \frac{EA}{60L^2} \begin{bmatrix} 0 & -3L\bar{\beta} + 36\tilde{v} & -(4L\bar{\beta} - 5\beta_2 L - 3\tilde{v})L & 0 & 3L\bar{\beta} - 36\tilde{v} & (L\bar{\beta} - 5\beta_2 L + 3\tilde{v})L \\ 0 & 72\tilde{u} & 6\tilde{u}L & 0 & -72\tilde{u} & 6\tilde{u}L \\ 0 & 6\tilde{u}L & 8\tilde{u}L^2 & 0 & -6\tilde{u}L & -2\tilde{u}L^2 \\ 0 & 3L\bar{\beta} - 36\tilde{v} & (4L\bar{\beta} - 5\beta_2 L - 3\tilde{v})L & 0 & -3L\bar{\beta} + 36\tilde{v} & -(L\bar{\beta} - 5\beta_2 L + 3\tilde{v})L \\ 0 & -72\tilde{u} & -6\tilde{u}L & 0 & 72\tilde{u} & -6\tilde{u}L \\ 0 & 6\tilde{u}L & -2\tilde{u}L^2 & 0 & -6\tilde{u}L & 8\tilde{u}L^2 \end{bmatrix} \quad (32)$$

$$K_v = \frac{\rho \dot{\psi}^2}{210} \begin{bmatrix} -70AL & 0 & 0 & -35AL & 0 & 0 \\ & -156AL + 504I/L & -22AL^2 + 42I & 0 & -54AL - 504I/L & 13AL^2 + 42I \\ & & -4AL^3 + 56LI & 0 & -13AL^2 - 42I & 3AL^3 - 14LI \\ & & & -70AL & 0 & 0 \\ & \text{sym} & & & -156AL + 504I/L & 22AL^2 - 42I \\ & & & & & -4AL^3 + 56LI \end{bmatrix} \quad (33)$$

Fig. 3   Transverse deflection of the beam tip using the deflection-only, linear EBv (——), nonlinear CLv (– – –) axially coupled Luv (–·–), and nonlinear NL (· · · ·) FE models.

the beam using the assumption of steady-state values for the axial displacement u, as described previously.[6] This leads to uncoupled transverse and axial displacements equivalent to Eq. (23). Moreover, the latter is assumed time independent and known for a given rotation velocity so that is not considered as variable in the finite element model. This reduces the nonlinear finite element model to four degrees of freedom, $\hat{q}^T = [v_1, \beta_1, v_2, \beta_2]$, for which the rows and columns corresponding to the axial displacement in mass and stiffness matrices may be eliminated. Additionally, the stiffness matrix K_a, the gyroscopic matrix G, and the force vector F_v vanish.

Because the axial displacement u, or the centrifugal load P, is assumed known for a given rotation velocity $\dot{\psi}$, the geometric stiffening matrix may be rewritten through discretization of Eq. (18), with Eq. (19), leading to

$$\hat{K}_g = \frac{\rho A L \dot{\psi}^2}{420} \begin{bmatrix} 180 & 6L & -180 & 27L \\ & 24L^2 & -6L & -4L^2 \\ & & 180 & -27L \\ \text{sym} & & & 10L^2 \end{bmatrix} \quad (36)$$

Note that, for this model, the geometric stiffening matrix always leads to an increase in the bending stiffness because the beam is subjected to an axial load $P(x)$ assumed to be always positive, that is, a centrifugal traction load.

The corresponding equations of motion may then be written as

$$(\hat{M}_t + \hat{M}_r)\ddot{\hat{q}} + (\hat{K}_e + \hat{K}_g + \hat{K}_v)\hat{q} = \hat{F}_a \quad (37)$$

D.   Centrifugal Loads Model Without Geometric Stiffening

The fourth finite element model [Euler–Bernoulli with only v as variable (EBv)] is derived from the preceding one by neglecting the geometric stiffening matrix $\hat{K}_g$. This leads to a decrease in the bending stiffness of the beam as the rotation velocity increases as shown earlier. Thus, the discretized equations of motion are

$$(\hat{M}_t + \hat{M}_r)\ddot{\hat{q}} + (\hat{K}_e + \hat{K}_v)\hat{q} = \hat{F}_a \quad (38)$$

Note from Eq. (38) that, because K_v is proportional to $\dot{\psi}^2$ and such that its diagonal elements are negative, there exists a limit value $\dot{\psi}_{\text{lim}}^2$ for the rotation velocity such that the diagonal elements of the global stiffness matrix $\hat{K}_e + \hat{K}_v$ become negative:

$$\dot{\psi}_{\text{lim}}^2 = \frac{210EI}{\rho L^2(AL^2 - 14I)} \quad (39)$$

In the next section, the four finite element models presented are compared through a numerical example.

V.   Numerical Comparison of Finite Element Models

To compare the proposed finite element models, a cantilever beam undergoing prescribed high-speed large rotations about its clamped end is considered. The material and geometrical properties of the beam are Young's modulus $E = 79.8$ GPa, mass density

$\rho = 2690\,\text{kgm}^{-3}$, width $b = 25$ mm, thickness $h = 4$ mm, and length $L = 400$ mm. The clamped base of the beam is subjected to a velocity profile as follows:

$$\dot{\psi} = \begin{cases} 50t, & \text{if} \quad 0 \le t < 1 \\ 50(2 - t), & \text{if} \quad 1 \le t < 2 \\ 0, & \text{if} \quad 2 \le t \end{cases} \quad (40)$$

The equations of motion resulting of the four finite element (FE) models, with five equally spaced elements along the beam, were numerically integrated using a MATLAB® ODE algorithm based on the trapezoidal rule with a free interpolant (ode23t). Note that the NL and Luv models leads to 15 global degrees of freedom, whereas CLv and EBv lead to only 10 because there are no axial displacements. In what follows, the results for the beam tip axial and transverse displacements are compared.

Figure 3 shows the transverse deflection of the beam tip using the deflection-only linear EBv (solid line) and nonlinear CLv (dashed line) and the axially coupled Luv (dash–dotted line) and NL (dotted line) FE models. Note that all models yield very similar results. The behavior of the beam motion may be divided in three parts. Initially, up to 1 s, the base of the beam is rotating with linearly increasing angular velocity [see Eq. (40)]. Hence, the mean transverse deflection of the beam tip is negative. The instantaneous acceleration of the base leads also to transient transverse vibrations, which are damped after 0.5 s due to an a posteriori damping of $C = 0.01I$.

Although the appearance of the transverse deflection is the same for all models in Fig. 3, the error of the simplified models EBv, CLv, and Luv compared to the NL results is not small. Figure 4 shows the transverse deflection error of the beam tip using the EBv (solid line), CLv (dashed line), and Luv (dash–dotted line) models compared to the NL model. Note that the error highly increases during transient transverse vibrations of the beam. It is also possible to see in Fig. 4 that the CLv model leads to smaller errors for $0.5 < t < 1$. This is because, in this period of time, the transverse vibrations are damped such that they do not induce axial vibrations. Hence, the axial displacement is only due to the traction induced by centrifugal load and, in this case, the assumption of steady-state axial displacements used to obtain the geometric stiffening in CLv model is valid. However, during transient transverse vibrations, this model leads to higher errors than the other models, which do not account for geometric stiffening because in this case there are induced axial vibrations.

The axial displacements of the beam tip were also evaluated using the linear Luv and NL axially coupled models. The results are presented in Fig. 5. Observe that the Luv model leads to a parabolic behavior of the axial displacement in the ranges $0 \le t < 1$ and $1 \le t < 2$. This is in agreement with the notion that, for this model, u is linear in $\dot{\psi}^2$ because it is subjected to the centrifugal load only, that is, the transverse deflections do not induce axial displacements. On the contrary, for the NL model, one may observe a large effect of transient transverse deflections on the axial displacements. When
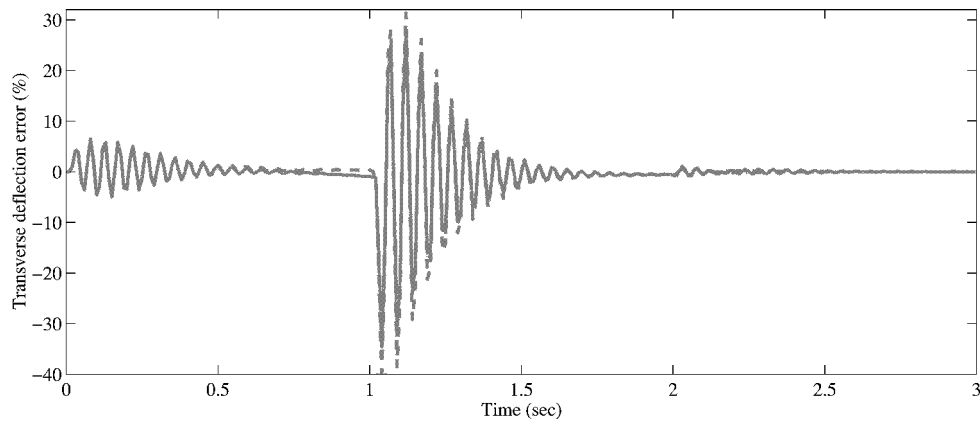
Fig. 4 Error in the transverse deflection of the beam tip using the EBv (——), CLv (– – –), and Luv (–·–) models compared to the NL model.
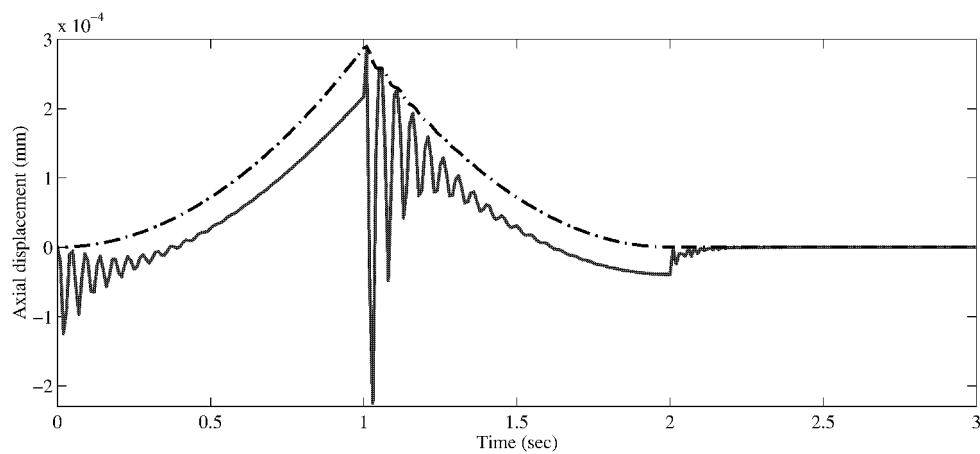

Fig. 5 Axial displacement of the beam tip using the axially coupled Luv (–·–) and NL (——) FE models.
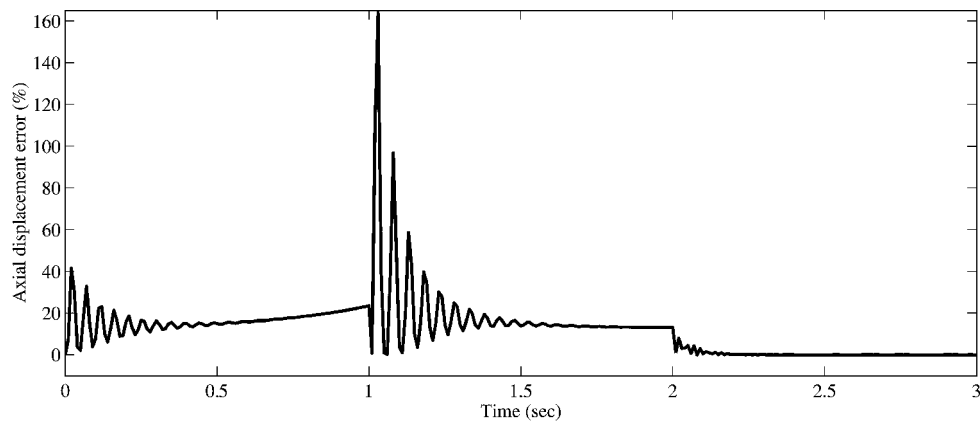

Fig. 6 Error in the axial displacement of the beam tip using the axially coupled, Luv FE model compared to the NL model.

transient transverse vibrations are damped, that is, for $0.5 < t < 1$ and $1.5 < t < 2$, there is still a considerable difference between the two models. This is due to the mean transverse deflection due to rotation (see these time periods in Fig. 3), which, although similar for both models, induces a corresponding axial displacement only for NL model. Hence, whereas for Luv the axial displacement is only due to centrifugal traction load, for NL, it is due to a combination of centrifugal load and transverse deflection.

Figure 6 presents the error in the axial displacement of the beam tip using the linear Luv model as compared to the NL model. Note that it is very large, as expected.

The error of the axial displacements using the Luv model is better noticed in a phase-plane graph. Hence, Fig. 7 presents the axial dis-

placement phase planes using NL (Fig. 7a) and Luv (Fig. 7b) models. To provide better understanding of the graph, the phase planes are divided in three regions corresponding to the three time periods, that is, $0 \leq t < 1$ (dash–dotted line), $1 \leq t < 2$ (dashed line), and $2 \leq t < 3$ (solid line). In Fig. 7a, note that there is some damped axial vibration around $u \approx -0.05$ μm initially, which is then followed by a motion at lower velocity to approximately 0.2 μm (dash–dotted line). Thereafter, the change in sign of the rotation acceleration at $t = 1$ s leads to transverse vibration, inducing damped axial vibration at large velocities (up to $\pm$ 40 μm/s), as shown in Fig. 7a, this time around 0.1 μm (dashed line). In the final stage of the motion, there are small axial vibrations tending to vanish (solid line). Using an analysis similar to the results of the Luv model (Fig. 7b), observe
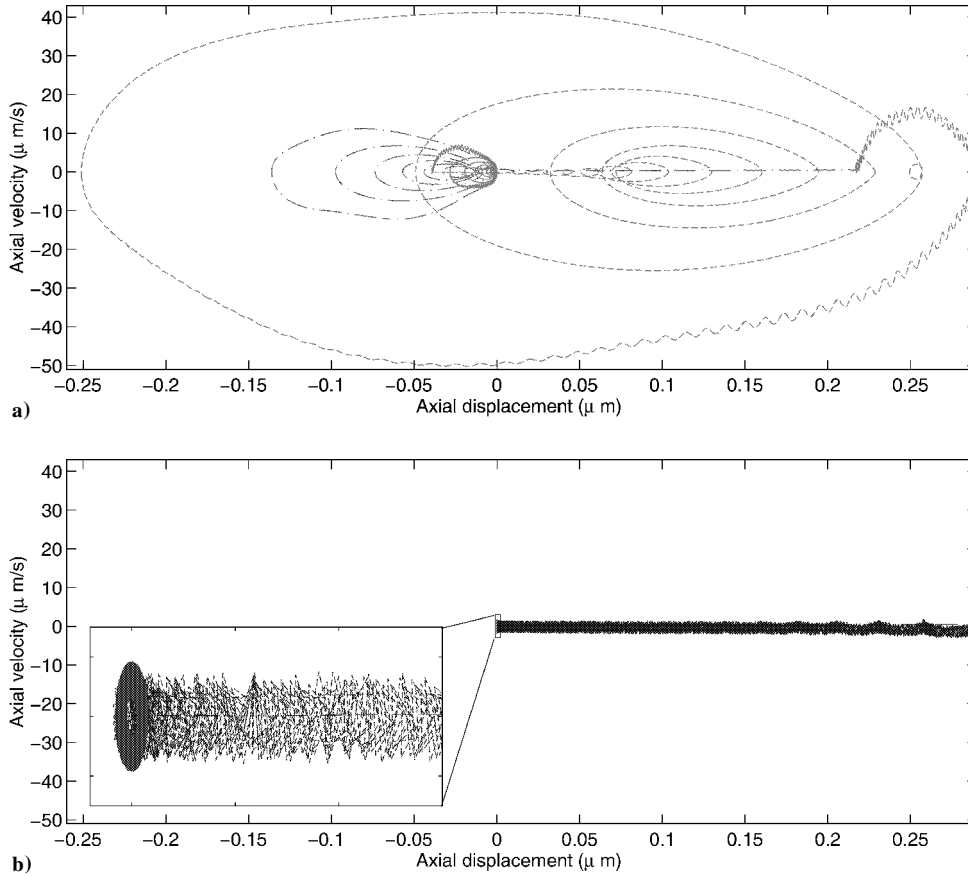
Fig. 7 Phase planes for the axial displacement of the beam tip at $0 \le t < 1$ (–·–), $1 \le t < 2$ (– – –), and $2 \le t < 3$ (——) using a) NL FE model and b) linear Luv FE model.
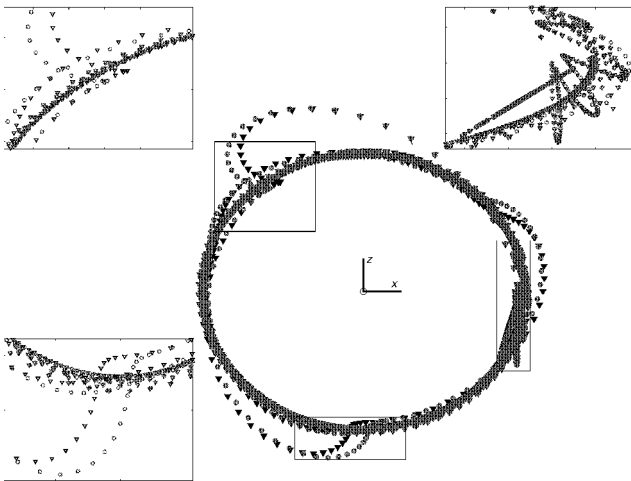

Fig. 8 Orbit of beam tip using NL (circles) and linear Luv (triangles) FE models.

that the axial displacements move from zero to the maximum value of approximately 0.3 μm (dash–dotted line) then returns to zero (dashed line) and presents very small oscillations around zero (solid line). Note, however, that the velocities are much smaller than for the NL model.

Figure 8 shows the orbit of the beam tip, that is, the trajectory formed by its position in the global xz frame, using NL (circles) and Luv (triangles) FE models for which displacements were amplified 700 times. Some areas were zoomed to provide better understanding of axial and transversal displacements effects. The left-hand side insets illustrate the difference between the results for the beam tip position using the linear and nonlinear models when the angular acceleration changes sign $t \approx 1$ s. The right zoomed area inset

corresponds to the initial and final oscillations when the base of the beam is around $\psi = 0$.

One of the main problems of using a linear model (Luv) to describe the beam undergoing large rotations is that, although transverse deflections are almost satisfactorily represented, not all behaviors are correctly evaluated. To illustrate this, the axial stress in the neutral line of beam tip element is shown in Fig. 9. Note that the Luv model yields always positive axial stress, corresponding to the traction due to the centrifugal load. Nevertheless, the NL model yields a highly cyclic stress, which is almost always compressive and up to 10 times higher than that for the linear model. Hence, although the NL model accounts for both traction due to centrifugal load and compression due to transverse deflection, contrary to what is predicted by the linear model, one observes that the resulting effect is a compression of the beam. This may be of main importance in structural integrity analysis.

Figure 10 presents the axial stress in the neutral line using the axially coupled Luv and NL FE models for two different instants of time. Note that linear and nonlinear models may yield quite different results for the axial stress state along the beam length. During the first oscillations due to the initial angular acceleration of the beam, the linear model predict traction over the entire beam length (Fig. 10a), whereas the results obtained with the nonlinear model show compression in almost all beam elements. Indeed, because axial stress in the neutral line is only due to centrifugal load in the linear model, it leads to positive axial stress increasing from beam tip to clamped end at all instants of time (Figs. 10a and 10b, linear). The same qualitative behavior may be observed in Fig. 10b; however, the axial stress magnitudes are much higher. Figure 10 corresponds to time instant $t = 1.14$ s, during the oscillations induced by the change in sign of the beam angular acceleration. Although, with the use of both models the beam is stretched near the clamped end, note that only the nonlinear model is able to predict the compression state near the beam tip.
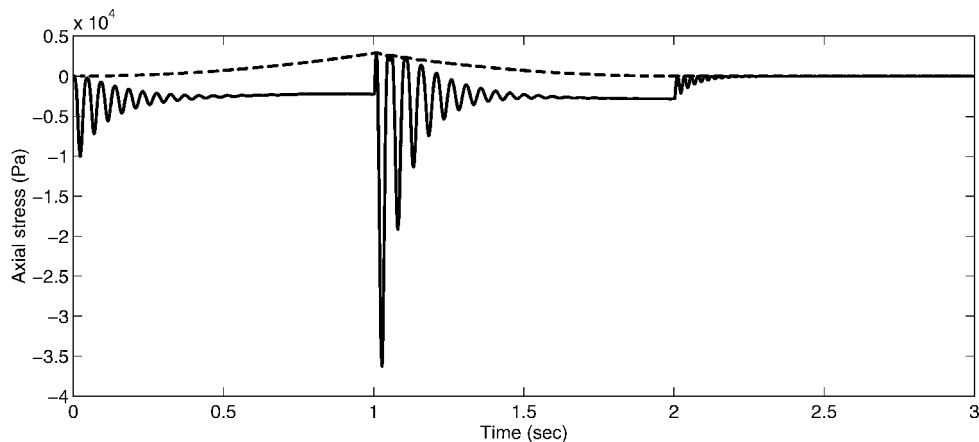
Fig. 9   Axial stress in the neutral line of beam tip element using the axially coupled Luv (- - -) and NL (——) FE models.

a) $t = 0.05$ s
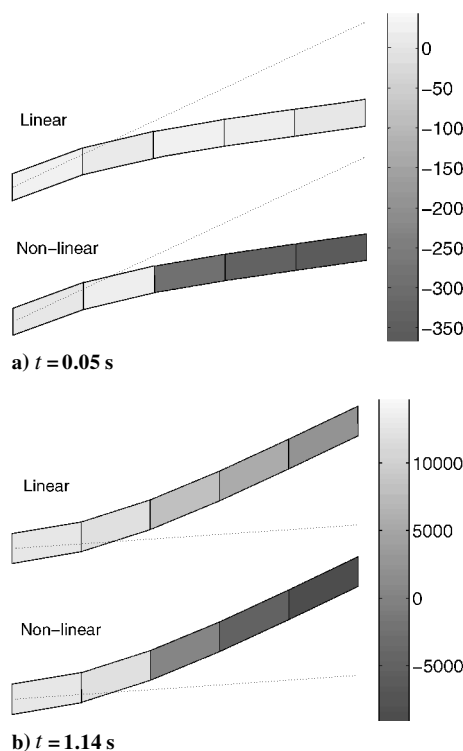

b) $t = 1.14$ s

Fig. 10   Axial stress (in pascal) in the neutral line using the axially coupled Luv and NL FE models.

VI.   Future Work

Future works are being directed to a numerical analysis of the full nonlinear model to study the influence of each nonlinear term in the correct description a rotating beam with time-varying angular velocity. A geometrically exact model proposed by Rochinha and Sampaio,[16] and then applied to nonlinear whirling of rods,[17] together with a singularity-free rotation representation,[18] will also be considered for a three-dimensional analysis. Thereafter, generalization of these studies for twisted or curved[19] beams are proposed. These models will also be extended to a flexible robot manipulator arm with prismatic joint[20−22] to study an axially controlled arm, that is, a sliding beam with controlled deployment and retrieval.

VII.   Conclusions

This work has presented a brief review of the open literature on the geometric stiffening of rotating flexible beams. Some of the several methodologies proposed in the literature to account for the stiffening effect in the dynamics equations were analyzed. Then, a general nonlinear model was formulated using a nonlinear strain–displacement relation, accounting for Coriolis force and coupling between extensional and flexural vibrations. This model was then used to analyze deeply simplified models found in the literature. In particular, the assumption of steady-state values for the centrifugal load was analyzed, and its consequences were discussed. Thereafter, four finite element models were proposed, one based on nonlinear theory and three on simplified linear theories. These models were then applied to the study of a flexible beam undergoing prescribed high-speed large rotations.

It was shown, through a frequency analysis, that the small deformations/large displacements approach together with assumptions of steady-state values for the axial displacement could be sufficient to capture the geometric stiffening due to rotation. However, this would only be realistic for constant angular velocity $\dot{\psi}$ and in the presence of damping to dissipate axial displacement due to initial angular acceleration. Hence, for the general case, it is suggested to keep nonlinear equations without the assumptions on axial displacement. The justification for keeping the term $(u'_0)^2$ in the strain–displacement relation is that, for this special case of the rotating beam, one should agree that, for large enough angular velocities, axial strains u'_0 may not be negligible compared to v'.

References

[1]Kane, T. R., Ryan, R. R., and Banerjee, A. K., "Dynamics of a Cantilever Beam Attached to a Moving Base," *Journal of Guidance, Control, and Dynamics*, Vol. 10, No. 2, 1987, pp. 139–151.

[2]Simo, J., and Vu-Quoc, L., "The Role of Non-Linear Theories in Transient Dynamic Analysis of Flexible Structures," *Journal of Sound and Vibration*, Vol. 119, No. 3, 1987, pp. 487–508.

[3]Choi, S. B., Cho, S. S., Shin, H. C., and Kim, H. K., "Quantative Feedback Theory Control of a Single-Link Flexible Manipulator Featuring Piezoelectric Actuator and Sensor," *Smart Materials and Structures*, Vol. 8, No. 3, 1999, pp. 338–349.

[4]Góes, L. C. S., and Adade Filho, A., "Robust Control of a Slewing Flexible Structure," *Applied Mechanics in the Americas*, edited by D. Pamplona, P. B. Gonçalves, C. Steele, I. Jasiuk, H. I. Weber, and L. Bevilacqua, AAM/ABCM, Rio de Janeiro, Brazil, Vol. 8, 1999, pp. 1139–1142.

[5]Schilhansl, M. J., "Bending Frequency of a Rotating Cantilever Beam," *Journal of Applied Mechanics*, Vol. 25, 1958, pp. 28–30.

[6]Sharf, I., "Geometric Stiffening in Multibody Dynamics Formulations," *Journal of Guidance, Control, and Dynamics*, Vol. 18, No. 4, 1995, pp. 882–890.

[7]Kuo, C.-F. J., and Lin, S.-C., "Discretization and Computer Simulation of a Rotating Euler–Bernoulli Beam," *Mathematics and Computers in Simulation*, Vol. 52, No. 2, 2000, pp. 121–135.

[8]Padilla, C. E., and von Flotow, A. W., "Nonlinear Strain–Displacement Relations and Flexible Multibody Dynamics," *Journal of Guidance, Control, and Dynamics*, Vol. 15, No. 1, 1992, pp. 128–136.

[9]Hanagud, S., and Sarkar, S., "Problem of the Dynamics of a Cantilever Beam Attached to a Moving Base," *Journal of Guidance, Control, and Dynamics*, Vol. 12, No. 3, 1989, pp. 438–441.

[10]London, K. W., "Comment on 'Dynamics of a Cantilever Beam Attached to a Moving Base,'" *Journal of Guidance, Control, and Dynamics*, Vol. 12, No. 2, 1989, pp. 284–286.

[11]Banerjee, A. K., and Dickens, J. M., "Dynamics of an Arbitrary Flexible Body in Large Rotation and Translation," *Journal of Guidance, Control, and Dynamics*, Vol. 13, No. 2, 1990, pp. 221–227.

[12]Linkins, P. W., Barbera, F. J., and Baddeley, V., "Mathematical Modeling of Spinning Elastic Bodies for Model Analysis," *AIAA Journal*, Vol. 11, 1973, pp. 1251–1258.

[13]Oguamanam, D. C. D., and Heppler, G. R., "Geometric Stiffening of Timoshenko Beams," *Journal of Applied Mechanics*, Vol. 65, No. 4, 1998, pp. 923–929.

[14]Wallrapp, O., and Schwertassek, R., "Representation of Geometric Stiffening in Multibody System Simulation," *International Journal for Numerical Methods in Engineering*, Vol. 32, No. 8, 1991, pp. 1833–1850.

[15]Urruzola, J., Celigueta, J. T., and de Jalon, J. G., "Generalization of Foreshortening Through New Reduced Geometrically Nonlinear Structural Formulation," *Journal of Guidance, Control, and Dynamics*, Vol. 23, No. 4, 2000, pp. 673–682.

[16]Rochinha, F. A., and Sampaio, R., "A Consistent Approach to Treat the Dynamics of Flexible Systems," *Journal of the Brazilian Society of Mechanical Sciences*, Vol. 19, No. 2, 1997, pp. 228–241.

[17]Huichala, F. C. C., Sampaio, R., and Rochinha, F. A., "The Nonlinear Whirling of Rods: A Numerical Investigation," *European Congress on Computational Methods in Applied Sciences and Engineering*, edited by E. Oñate, G. Bugeda, and B. Suárez [CD-ROM], ECCOMAS, Barcelona, 2000.

[18]Trindade, M. A., and Sampaio, R., "On the Numerical Integration of Rigid Body Nonlinear Dynamics in Presence of Parameters Singularities," *Journal of the Brazilian Society of Mechanical Sciences*, Vol. 23, No. 1, 2001, pp. 49–62.

[19]Park, J.-H., and Kim, J.-H., "Dynamic Analysis of Rotating Curved Beam with a Tip Mass," *Journal of Sound and Vibration*, Vol. 228, No. 5, 1999, pp. 1017–1034.

[20]Vu-Quoc, L., and Li, S., "Dynamics of Sliding Geometrically-Exact Beams: Large Angle Maneuver and Parametric Resonance," *Computer Methods in Applied Mechanics and Engineering*, Vol. 120, No. 1–2, 1995, pp. 65–118.

[21]Trindade, M. A., and Sampaio, R., "Influence of Flexibility in the Dynamics of Multibody Systems," *Proceedings of the 3rd Asian-Pacific Conference on Computational Mechanics*, edited by C.-K. Choi, C.-B. Yun, and D.-G. Lee, Vol. 2, Techno-Press, Seoul, Republic of Korea, 1996, pp. 943–948.

[22]Riquelme, R., and Sampaio, R., "Symbolic and Numeric Programming in Dynamics," *European Congress on Computational Methods in Applied Sciences and Engineering*, edited by E. Oñate, G. Bugeda, and B. Suárez [CD-ROM], ECCOMAS, Barcelona, 2000.